ORIGINAL PAPER

Twinning Behavior in Uphill Nano-Tribological Process

Yougui Liao

Abstract Twinning behavior in the contact region between two tips is for the first time observed in a nano-tribological process. An Au (gold) polycrystalline tip, formed in TEM system, slides uphill on a W (tungsten) tip, mechanically inducing an Au polycrystalline transition layer. Not only does the tensile stress gradient initialize the twin formation but also the direction of the first sliding step determines the crystalline orientation of the first primary twin due to the lowest surface energy of FCC Au {111} planes. The crystalline orientation of the second primary twin is aligned with the first primary twin by coherent twin boundary regardless of the sliding direction and stress distribution. A triple boundary junction, between the Au tip, Au transition layer and vacuum is a favorable configuration probably due to the lowest energy of the system. On the other hand, defective crystalline phase is formed in the compressive region. It is proposed that crystalline rotation and active disclination dipoles are mainly responsible for the movement of twin boundary during the Au tip sliding process.

Keywords Twinning · Tip sliding · Sliding direction · Stress gradient · Crystalline rotation · Nano-tribology · In situ TEM

1 Introduction

When a single asperity touches and slides on surface, complex phenomena can occur: local rearrangement of atoms in the contact region [1] and permanent change of the surface structure [2]. Many models have been proposed to explain fundamental nano-tribological properties. One of the most common models is generation and movement of dislocations at the interface between two single crystalline materials during sliding. [1] Unfortunately, polycrystalline surfaces rather than single crystalline surfaces are the most common case in reality. On the other hand, all those models assume that the sliding surfaces are flat. However, the asperity can slide both "uphill" and "downhill" due to surface roughness. Here, the terms "uphill" and "downhill" processes indicate the relative sliding directions, meaning "uphill" sliding causes a compressive contact stress while "downhill" sliding causes a tensile contact stress.

Grain rotation has been proposed to be a mechanism in nanocrystalline materials during crystal growth [3–5], thin film deposition [6], thermal annealing process [7], high-pressure torsion (HPT) process [8], in situ TEM stressing [9], and deformation [10]. The grain rotation minimizes interfacial energy, strain energy stored by dislocations, and unbalanced forces [11–13]. Observation suggested that grain rotation converts large angle grain boundaries (LAGB) to small angle grain boundaries (SAGB), forming larger grains. [6, 8] The SAGBs are close to their energy minimum. However, the rotation angle normally is very small, e.g., 1° reported [6]. One reason is that the fully enclosed grains in a matrix cannot freely rotate without constraint because each grain is attached at the grain boundaries (GBs) of the other grains. Profuse nano-scale twins in width of ≤20 nm had also been observed in mechanically deformed materials, e.g., refer to [14]. The other deformation phenomenon highlighted here is generation of disclination dipoles. The disclination dipoles are created when the stress at the grain boundary is large enough. [15, 16]

Y. Liao (✉)
Department of Materials Science and Engineering, Northwestern University, Evanston, IL 60208, USA
e-mail: yougui.liao@globalsino.com

In many cases, the study of the contact region between two sliding solids is incorrect because this contact region has been destroyed if post-mortem (ex-situ) TEM analysis is performed. Moreover, because this region is buried, very few direct observations of microstructural change in the contact region have been performed. Related studies have been done using in situ transmission electron microscopy (TEM) by controlling the temperature and/or stress on polycrystalline materials, enabling the study of dynamic phenomena [17, 18]. They have used a strain-holder (with or without heating) mounted inside the TEM system [19–21]. More relevant, in situ nanoindentation studies have been performed, for instance inducing grain growth in polycrystalline Al (aluminum) materials [18]. For a recent review of relevant in situ studies see Refs. [22, 23].

In this study, an Au polycrystalline tip, formed in TEM system, slides uphill on a bigger W tip, mechanically inducing an Au transition layer and initializing crystalline orientation of the first primary twin. The tensile stress gradient determines the formation of the first primary twin. A {111} plane of this twin is aligned in parallel to the sliding direction of the first sliding step. The crystalline orientation of the second primary twin is subsequently aligned with the first primary twin by coherent twin boundary regardless of the sliding direction and stress distribution. The formed twins' exhibit multiple twin configuration [16, 24] Grain rotation occurs in both tensile and compressive region, while twin boundary (TB) moves significantly at the boundary between the two regions. The observed maximum crystalline rotation angle is the misorientation angle between the two twins and is very large ($\sim 14.6°$). In the compressive region, a single crystalline grain is formed due to grain rotation. The driving force here is the rotational configurational force. Moreover, the first primary twin can also grow atomically layer-by-layer other than discontinues grain rotation. The experimental results also indicate that a triple junction between the Au transition layer, the Au tip, and the vacuum is the minimum energy configuration.

2 Experimental Details

A nanocrystalline Au tip was created by a freestanding Au film sliding on a W tip inside TEM system. The Au film in thickness of 18 nm was prepared by physical sputtering of pure gold (99.9 %) onto a sodium chloride substrate (NaCl) at room temperature. The deposition was performed at a pressure of 10^{-5} torr and a deposition rate of ~ 0.5 nm/s. To suppress columnar grain structure, the deposition was interrupted for 1 min at ~ 3 nm thickness intervals during the film growth. The Au film was released by dissolving the NaCl substrate away to obtain unsupported thin Au films

floating in water. The freestanding thin films were then manually collected on 300 mesh TEM Cu (copper) grids (from Ted Pella, Inc). The grain size in the Au films was less than 20 nm and was about 9 nm on average. The in situ tribological experiments were performed in a Tecnai F20 G2 TEM system operated at 200 keV. HRTEM (high-resolution transmission electron microscopy) images were acquired using a Gatan CCD camera.

The W tip was prepared by a standard electrochemical polishing method using a buffered NaOH solution. The radius of the curvature of the W tip surface was about 37 nm. The in situ TEM holder (a HS100 STM-TEM-Holder^TM, Nanofactory Instruments) had been described elsewhere [25]. The Au tip was driven at a step resolution of 0.5 nm. The sliding process was performed in the direction of the trace shown in the schematic in Fig. 1: (i) The sliding direction of the Au tip from step 0–27 remained unchanged; (ii) The Au tip was slightly retracted from step 28 to 33; (iii) The Au tip slid again from step 34 to 35. The curve in the inset indicates the stress distribution in the contact region from sliding step 0 to step 27: tensile (positive) and compressive (negative) stresses. The black spot shows the approximate position of the twin boundary (TB-B) between the first and second primary twins.

3 Results

The HRTEM image in Fig. 2 shows the Au film and W tip before they touched and slid against each other. At this stage, the Au tip was not formed yet. The lattice fringes in the Au film indicate that no transition layer was established at the edge of the film at this stage. The moving direction of the Au materials during the sliding process is marked by the white arrow in the figure.
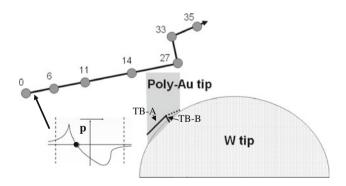

Fig. 1 Schematic shows the entire tribological process. The area between the two *dash lines* indicates the stress distribution in the Au transition layer. TB-A and TB-B ware twin boundaries discussed below. The *curve* represents the stress distribution in the transition layer. Tensile stress is applied at $p > 0$, while compressive stress is applied at $p < 0$. The *black dot* on the curve indicates the approximate location of TB-B
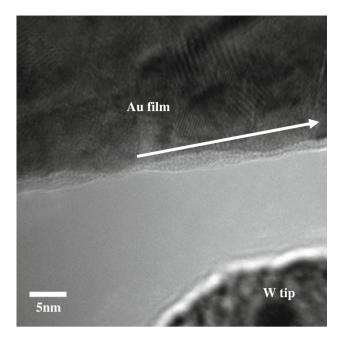
Fig. 2 HRTEM image before the Au film and W tip touched and slid against each other. The *white arrow* indicates the sliding direction of the Au materials. The W tip is out of focus at this stage

The thickness of the Au film, ~ 18 nm, is smaller than the thickness of the W tip, ~ 74 nm. Figure 3a schematically shows that the Au tip was formed and slid on the bottom side of the W tip. As indicated by the black vertical solid line, the edge of the Au tip overlapped with the edge of the W tip relative to the direction of the electron beam in the TEM system. The TEM image in Fig. 3b shows that an Au transition layer between the Au and W tips was established at the first sliding step. This transition layer was established within less than 0.03 s. This layer contained 8
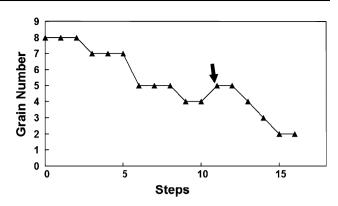

Fig. 4 Change of grain number in the Au transition layer at sliding step 1 to 16

nanocrystalline Au grains, marked by the dashed gray curves, in size ranged from ~ 5 to ~ 15 nm similar to the size distribution in the as-prepared Au film. The sliding direction of the Au tip is indicated by the long white arrow. The (111) plane (as indicated in the inset) of the first grain located at the edge of the transition layer, marked by the asterisk, was aligned by the sliding force in parallel to the sliding direction. The optical axis of the TEM system remained unchanged in the entire tribological process and was slightly tilted off [011] zone axis of the first grain, and thus the $(\bar{1}1\bar{1})$ plane, marked by the short white line was also slightly tilted off the optical axis.

The Au grain number in the transition layer mainly decreased during the sliding process as shown in Fig. 4. For instance, one grain first disappeared at sliding step 3. After sliding step 15, there were only two grains left as shown in Fig. 5. That is, only a single grain II existed in the compressive region. It is necessary to mention that the
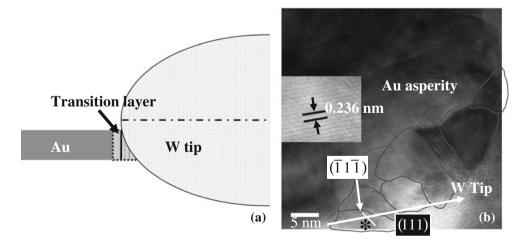

Fig. 3 a Schematic shows that the Au tip slid on the W tip. There was a transition layer, enclosed by the *dashed line*, established between the Au and W tips. **b** TEM image shows the Au transition layer formed at the first sliding step within 0.03 s. There are 8 Au

nanocrystalline grains in the translation layer. The established (111) plane of the first primary grain, marked by the *asterisk*, was exactly in parallel to the sliding direction indicated by the *long white arrow*
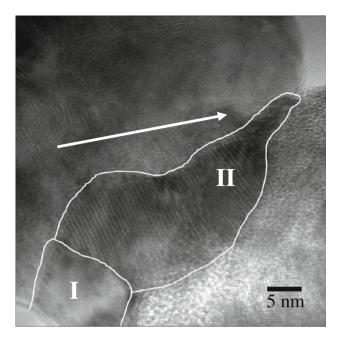
Fig. 5 There were only two grains left after sliding step 15. Again, the *long white arrow* indicates the sliding direction of the Au tip

grain number increased at sliding step 12, indicated by the arrow in Fig. 4.

By comparing Fig. 6a with b, it can be known that grain 8 grew at sliding step 5. The difference of the fringe contrast of grain II also indicates that the grain rotated at the same time. The grain rotation of grain II tended to align one of its {111} planes to match (111) plane of grain I. Sliding step 6 completed this matching process (not shown) and a clear TB was formed at the boundary (($\bar{1}1\bar{1}$) plane)

between the tensile and compressive regions indicated by a dashed line in Fig. 6b.

One junction between the two twin boundaries, ($11\bar{1}$) (TB-A) and ($\bar{1}1\bar{1}$) (TB-B), were formed as shown in Fig. 7. In the entire tribological process, TB-B moved and TB-A extended in the sliding direction, respectively, resulting in the junction following the edge of the Au tip. It should be mentioned that the crystalline orientation of region II' was determined by the crystalline orientation of twin I, which can be explained by CSL (Coincident site lattice) theory. That means the crystalline orientation of twin II' was aligned with twin I by coherent twin boundary regardless of the sliding direction and stress distribution. TB-B did not follow the left edge of the Au tip when the Au tip was retracted from the W tip as shown in Fig. 7b, taken at the end of the retracting process (step 33). However, when the Au tip slid again, as indicated in Fig. 7c, the triple junction caught up with the left edge of the Au tip again even though TB-B did not fully follow this movement. At sliding step 35, both triple junction and TB-B followed the movement of the Au tip.

Figure 8 shows the movement of TB-B along the W tip surface. The terraces indicate that TB-B did not move significantly at those sliding steps.

4 Discussion

To explain the phenomena described above, crystalline/grain rotation and generation of disclination dipoles occurring in mechanical deformation process should be introduced. It is suggested that grain rotation especially occurs in the
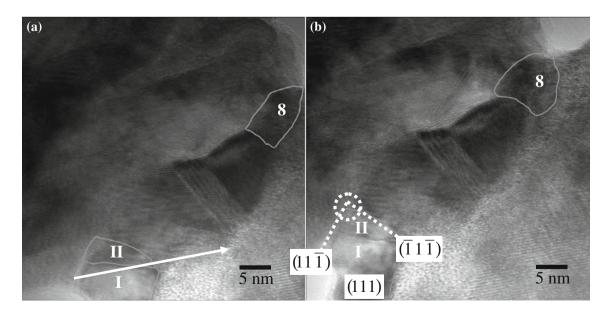

Fig. 6 **a** TEM image taken after sliding step 4. **b** TEM image, taken after slide step 5, shows that grain II rotated and grain 8 grew
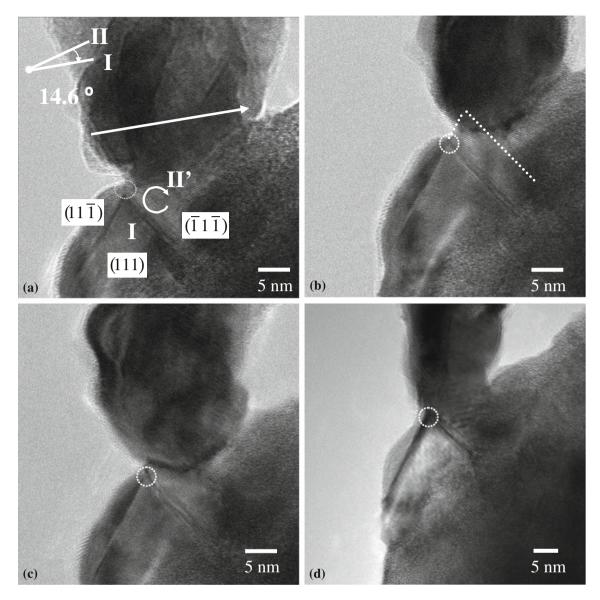
Fig. 7 TEM images taken after sliding step 27 (**a**), 33 (**b**), 34 (**c**), and 35 (**d**). The *dashed circle* indicates the triple junction between the Au transition layer, Au tip and vacuum
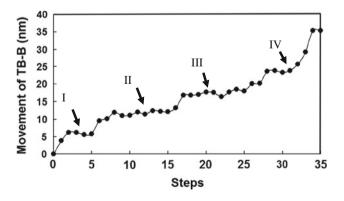

Fig. 8 The movement of TB-B along the W tip surface. The terraces, marked by the arrows, indicate that TB-B did not move significantly at those sliding steps

deformation process of nano-polycrystalline materials and can be induced by the torque formed in the sliding process [26]. For instance, Theissmann at al. [27] theoretically predicted lattice reorientation before the coalescence process of the poly-materials based on CSL theory. Both compressive [28] and tensile [10] deformations can induce grain rotation to form SAGBs in various polycrystalline materials. In general, the rotational degree of freedom is lower at smaller angle grain boundaries, inhibiting further crystalline orientation alignment between grains from forming a perfect crystalline grain. [29] In the present transition layer, the rotational degree of freedom is higher than that in bulk materials because most nanograins expose in the vacuum of the TEM system as shown in Fig. 3a, resulting in easier crystalline rotation.

The driving forces of grain rotation can be applied stress, relaxation of stress concentration [10], motion of dislocation [30], and the reduction of the total energy of surrounding grain boundaries [7, 30] stored by plastic deformation. Consequently, the rotation rate also depends on many factors [29, 31]. First, it was suggested that rotation rate is mostly proportional to configurational force. Second, grain rotation is size-dependent. Both theoretical simulation and experimental observation performed by Harris et al. [7] suggested that the rotation rate of grains in size of approximately 200 nm is very low at 2.4° per hour. Yeadon et al. [32] demonstrated that Cu (copper) particles could only be re-oriented by grain rotation when they were smaller than approximately 50 nm in size. Harris et al. [7] also presented grain rotation of Au polycrystalline materials, observed at room temperature using TEM. They suggested that grains in size below a certain value yields dependence of rotation rate on d^{-4}, where d is grain size [19]. In the present Au tip, the size of nanocrystalline grains ranges from ~ 5 to ~ 15 nm and 9 nm on average, resulting in significant grain rotation. For instance, grain rotation of Au particles at 9 nm in size is four orders of magnitude higher than those at 90 nm in size. Third, Harris et al. [7] also proposed that the rotation rate showed discontinuous change [27] and decreased with time under identical stresses. This decrease indicates the reduction of the driving force. The discontinuous rotation process, especially for small grains, can occur very quickly, for instance, Theissmann et al. [27] concluded that each rotational step took less than 0.04 s, based on in situ hot-stage TEM observation.

Besides grain rotation, mechanical stress can also induce formation and motion of wedge disclination dipoles, [33, 34], resulting in ultra fine crystalline grains from big grains and fascinating rotational plastic deformation. In the present tribological process, the rotation axis of the disclination dipoles is perpendicular to the plane, consisted of the Au and W tips and the Au transition layer. On the other hand, the dynamics of the Au transition layer is coupled by the tip sliding. The energy from the sliding tip can be stored in this layer in the form of strain energy. These stored strain energy triggers the generation of disclination dipoles and crystalline rotation and consequently leads to grain coalescences via decrease of GB angle or elimination of GBs.

The sliding process between Au nano-polycrystalline and W tips is summarized in Fig. 9. The Au nanograins distribute randomly in the initial Au film (Fig. 2) before the tips slide against each other as shown in Fig. 9a. Moreover, the engaging process of the Au film and W tip does not modify the nanograin distribution in the Au tip if the tips do not slide against each other. When the tips start sliding, the nanograins move away from the black dashed line as
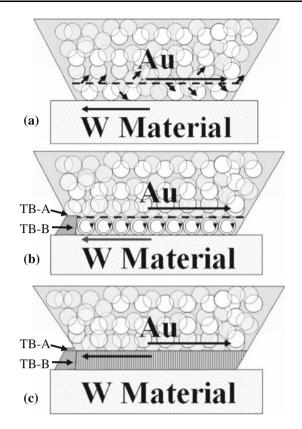

Fig. 9 Schematic shows: **a** The nanograins in the Au tip move to form a transition layer at the beginning of the first sliding step; **b** The tips slide against each other and the nanograins in the compressive region rotate during the sliding process; **c** A single grain is formed in the compressive region. The Au tip slides on the transition layer rather than directly on the W tip

shown by the black arrows in Fig. 9a, resulting in alignment of the grain boundaries along the line and forming a transition layer between the two tips.

The TEM image in Fig. 3b indicates that an Au transition layer, in thickness of ~ 15 nm, has been established, within less than 0.03 s, between the two tips at the first sliding step. This layer contains 8 nanocrystalline Au grains, in size ranged from ~ 5 to ~ 15 nm. Those grains can discontinuously rotate at the later sliding steps. Moreover, the lateral forces applied to the transition layer by the two tips, enhances the grain rotation due to grain-boundary slip [7, 19, 35, 36]. Atomic diffusion at grain boundaries also partially facilitates the grain rotation because the grains are not ideally in spherical shape. In the later sliding process, the orientation of the grain in the compressive region, e.g., Fig. 5, remains almost unchanged as schematically shown in Fig. 9c. The tribological sliding between the two tips mainly takes place at the interface between the Au tip and the Au transition layer.

From sliding steps 1–27, the stress in the transition layer is schematized in the curve, marked by asterisk, in Fig. 1 as the Au tip slides uphill. The compressive stress and its

gradient in the right part of transition layer enhance dynamic grain coalescence, similar to the phenomena describing that grain rotation converts LAGBs to small angle subgrain boundaries, forming large grains consisted of small angle subgrains. [6, 8]. This coalescence induces decrease of the grain number as shown in Fig. 4. At sliding step 11, the sliding process causes formation of disclination dipoles, resulting in grain refinement and increase of the grain number as shown by the arrow in Fig. 4. The TEM image in Fig. 5 indicates that a single grain is formed in the compressive region. This TEM contrast also indicates this grain is defective. From sliding step 15–27, the Au tip only slides on the single crystalline Au transition layer as mentioned above.

Figure 3 also shows the crystalline orientation of the first grain, marked by the asterisk. The sliding direction is indicated by the long white arrow in Fig. 3b. The interplanar spacing, parallel to the sliding direction, of the first grain is 0.236 nm as shown in the inset, corresponding to FCC Au (111) plane. That means the (111) plane of this grain is initially aligned exactly in the sliding direction. The alignment of the crystalline orientation is determined by the lowest surface energy because for FCC Au crystalline materials the configuration of surface energy is $\gamma_{(111)}$ (0.8 J/m^2) < $\gamma_{(110)}$ (1.28 J/m^2) < $\gamma_{(100)}$ (1.6 J/m^2) [37–39].

At the first sliding steps, large strain energy has been stored at the boundary between tensile and compressive regions as shown in Fig. 1. After sliding step 6, the stored energy is reduced by forming two twin boundaries in {111} planes, namely $(11\bar{1})$ (TB-A) and $(\bar{1}1\bar{1})$ (TB-B). The artificial broadening of two twin boundaries, as shown in Fig. 7, is because of the two {111} planes slightly tilt off the optical axis. TB-A extends in $(11\bar{1})$ plane and TB-B moves following the Au tip via diffusion and crystalline rotation. The moving speed of TB-B varies in the tribological process as shown in Fig. 8. This tribological behavior is different from the conventional atomic stick–slip mechanism [1]. Terrance I shows the average moving distance per step from sliding step 2 to 5 is negligible, originated from the fact that the movement of TB-B is suppressed by the large misorientation between grain II and grain I as shown in Fig. 6. However, the moving distance of TB-B at sliding step 6 is significantly large (~3.78 nm), which is close to the size of grain II (~3.47 nm). From sliding step 8 to 15 (terrace II), the average moving speed of TB-B is 0.289 nm/step (~1.26 atomic layers/step). That is, the twin boundary almost moves layer-by-layer, similar to deformation twinning observed by Han et al. [40]. As mentioned above, after sliding step 15, there is only a single grain in the compressive region. However, the moving speed of TB-B in this region is not constant, for instance, a big moving step

(~3.46 nm) occurs at sliding step 17. This can be due to formation of disclination dipoles followed by crystalline rotation, indicated by some models [34]. The formation location of disclination dipoles can be at defective locations in the single crystalline Au materials, which are not visible under HRTEM imaging condition. From sliding step 18 to 27, no grain rotation is caused and the average moving speed of TB-B is approximately 0.34 nm/step (~1.48 atomic layers/step).

In the retraction process from step 28 to 33, the junction between TB-A and TB-B does not fully follow the edge of the Au tip, e.g., as shown in Fig. 7b. However, the moving distance of TB-B is still significant; especially it is ~3.34 nm at step 28, because the retraction process provides much higher tensile stress to TB-B. The moving speed of TB-B is about 0.23 nm/step (~1 atomic layer/step) from retraction step 29 to 31. The maximum moving step of TB-B is ~6.7 nm, occurred at sliding step 34. At this sliding step, the Au crystalline materials, enclosed by the dashed lines in Fig. 7b, has rotated from crystalline orientation of twin II' to that of twin I. The rotation angle is very large (~14.6°).

Figure 10 shows the location of twin boundary TB-B relative to the left edge of the Au tip at different tribological stages. As shown in Fig. 10a, when the tip is wide (from ~24 to ~44 nm), TB-B is located at the boundary between the tensile and compressive regions, which is inside the Au tip, during the sliding process. In the retraction process as shown in Fig. 10b, the entire transition layer is under tensile stress and TB-B is located on the left of the tip. When the tip is narrow (from ~15 to ~24 nm), the triple junction between the Au tip, Au transition layer and vacuum locks TB-B during the sliding process as shown in Fig. 10c.

It is necessary to mention that no twin boundaries are formed if the Au tip does not slide on the W tip even though it retracts from the W tip after engaging. This phenomenon is consistent with the nanowire formation,
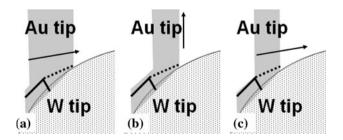

Fig. 10 Schematics show the location of twin boundary TB-B relative to the left edge of the Au tip: **a** TB-B is inside the Au tip when the tip is wide (from ~24 to ~44 nm); **b** TB-B is on the left of the tip; **c** The triple junction locks TB-B when the tip is narrow (from ~15 to ~24 nm)

from nano-polycrystalline Au film, carried out in situ TEM [41].

5 Conclusions

We have presented microstructural evolution in the contact region between the Au and W tips during the uphill sliding of the Au polycrystalline tip on the W tip. Large strain energy is stored in the contact as a result of the sliding force applied by the Au tip. This high-strain energy enhances formation of disclination dipoles and grain/crystalline rotation. Grain rotation induces grain coalescence in the compressive region. The configurational force, induced by the Au tip sliding and high-rotational degree of freedom of the nanograins facilitates the grain rotation, inducing motion of twin boundary and grain coalescence. It is very important that the crystalline orientation of the first primary twin in the transition layer is determined by the sliding direction regardless of the crystalline orientation of the W tip and the stress distribution. The orientation of the second primary twin is based on the crystalline orientation of the first primary twin, which can be explained by CSL (Coincident site lattice) theory. The discontinuous movement of twin boundary is observed due to discontinuous crystalline rotation and layer-by-layer atomic movement. Note that due to the scale limitation in TEM observation at high-spatial resolutions, it is not possible to perform continuous sliding processes at high-spatial resolution at large scale, which may be important for tribological process.

References

1. Liao, Y., Marks, L.D.: Modeling of thermal-assisted dislocation friction. Tribol. Lett. **37**, 283 (2010)
2. Wiesendanger, R., Guntherodt, H.-J.: Scanning Tunneling Microscopy III. Springer Series in Surface Science, vol. 29. Springer, Berlin (1996)
3. Moldovan, D., Yamakov, V., Wolf, D., Phillpot, S.R.: Scaling behavior of grain-rotation-induced grain growth. Phys. Rev. Lett. **89**, 206101 (2002)
4. Haslam, A.J., et al.: Stress-enhanced grain growth in a nanocrystalline material by molecular-dynamics simulation. Acta Mater. **51**, 2097 (2003)
5. Moldovan, D., Wolf, D., Phillpot, S.R., Haslam, A.J.: Role of grain rotation during grain growth in a columnar microstructure by mesoscale simulation. Acta Mater. **50**, 3397 (2002)
6. Pashley, D.W., Jacobs, M.H., Stowell, M.J., Law, T.J.: The growth and structure of gold and silver deposits formed by evaporation inside an electron microscope. Philos. Mag. **10**, 127 (1964)
7. Harris, K.E., Singh, V.V., King, A.H.: Grain rotation in thin films of gold. Acta Mater. **46**, 2623 (1998)
8. Wang, Y.B., et al.: Mechanism of grain growth during severe plastic deformation of a nanocrystalline Ni–Fe alloy. Appl. Phys. Lett. **94**, 011908 (2009)
9. Rankin, J., Sheldon, B.W.: In situ TEM sintering of nano-sized ZrO_2 particles. Mater. Sci. Eng. A **204**, 48 (1995)
10. Wang, Y.B., Li, B.Q., Suia, M.L., Mao, S.X.: Deformation-induced grain rotation and growth in nanocrystalline Ni. Appl. Phys. Lett. **92**, 011903 (2008)
11. Li, J.C.M.: Possibility of subgrain rotation during recrystallization. J. Appl. Phys. **33**, 2958 (1962)
12. Doherty, R.D., Szpunar, J.A.: Kinetics of subgrain coalescence—a reconsideration of the theory. Acta Metall. **32**, 1789 (1984)
13. Hermann, G., Gleiter, H., Baro, G.: Investigation of low energy grain boundaries in metals by a sintering technique. Acta Metall. **24**, 353 (1976)
14. Brown, T.L., Saldana, C., Murthy, T.G., Mann, J.B., Guo, Y., Allard, L.F., King, A.H., Compton, W.D., Trumble, K.P., Chandrasekar, S.: A study of the interactive effects of strain, strain rate and temperature in severe plastic deformation of copper. Acta Mater. **57**(18), 5491 (2009)
15. Zizak, I., Darowski, N., Klaumünzer, S., Schumacher, G., Gerlach, J.W., Assmann, W.: Grain rotation in nanocrystalline layers under influence of swift heavy ions. Nucl. Instrum. Methods Phys. Res. B **267**, 944 (2009)
16. Howie, A., Marks, L.D.: Elastic strains and the energy balance for multiply twinned particles. Philos. Mag. A **49**, 95 (1984)
17. Gianola, D.S., et al.: Stress assisted discontinuous grain growth and its effect on the deformation behavior of nanocrystalline aluminum thin films. Acta Mater. **54**, 2253 (2006)
18. Jin, M., Minor, A.M., Stach, E.A., Morris, J.J.W.: Direct observation of stress-Induced grain growth during the nanoindentation of ultrafine-grained Al at room temperature. Acta Mater. **52**, 5381 (2004)
19. Shan, Z., Stach, E.A., Wiezorek, J.M.K., Knapp, J.A., Follstaedt, D.M., Mao, S.X.: Grain boundary-mediated plasticity in nanocrystalline nickel. Science **305**, 654 (2004)
20. Legros, M., Gianola, D.S., Hemker, K.J.: In situ TEM observations of fast grain boundary motion in stressed nanocrystalline aluminum films. Acta Mater. **56**, 3380 (2008)
21. Milfigan, W.W., Hackney, S.A., Ke, M., Aifantis, E.C.: In Situ studies of deformation and fracture in nanophase materials. Nanostruct. Mater. **2**, 267 (1993)
22. Marks L.D., Warren O.L., Minor A.M., Merkle A.P.: Tribology in full view. MRS Bull. **33**, 1168 (2008)
23. Y. Liao, Practical electron microscopy and database (www.globalsino.com/EM/) (2006)
24. Myshlyaev, M.M., McQueen, H.J., Mwembela, A., Konopleva, E.: Twinning, dynamic recovery and recrystallization in hot worked Mg–Al–Zn alloy. Mater. Sci. Eng. A **337**, 121 (2002)
25. Merkle, A.P., Marks, L.D.: Liquid-like tribology of gold studied by in situ TEM. Wear **265**, 1864 (2008)
26. Heilmann, P., Clark, W.A.T., Rigney, D.A.: Orientation determination of subsurface cells generated by sliding. Acta Mater. **31**(8), 1293 (1983)
27. Theissmann, R., Fendrich, M., Zinetullin, R., Guenther, G., Schierning, G., Wolf, D.E.: Crystallographic reorientation and nanoparticle coalescence. Phys. Rev. B **78**, 205413 (2008)
28. Barrett, C.S., Lavenson, L.H.: The structure of aluminum after compression. Trans. Metall. Soc. AIME **137**, 112 (1940)
29. Martin, G.: Driving force and mobility for microstructural evolutions. Phys Stat Sol (b) **172**, 121 (1992)

30. Shewmon, P.G.: In: Margolin, H. (ed.) Recrystallization, Grain Growth and Textures, vol. 166. American Society of Metals, Metals Park (OH) (1966)

31. Cahn, John.W., Taylor, J.E.: A unified approach to motion of grain boundaries, relative tangential translation along grain boundaries, and grain rotation. Acta Mater. **52**, 4887 (2004)

32. Yeadon, M., et al.: In-situ observations of classical grain growth mechanisms during sintering of copper nanoparticles on (001) copper. Appl. Phys. Lett. **71**, 1631 (1997)

33. Romanov, A.E., Vladimirov, V.I.: In: Nabarro, F.R.N. (ed.) Dislocations in Solids, vol. 9, p. 191. North Holland, Amsterdam (1992)

34. Müllner, P., King, A.H.: Deformation of hierarchically twinned martensite. Acta Mater. **58**(16), 5242 (2010)

35. Raj, R., Ashby, M.F.: Grain boundary sliding and diffusional creep. Metal. Trans. **2**, 1113 (1971)

36. Moldovan, D., Wolf, D., Phillpot, S.R.: Theory of diffusion-accommodated grain rotation in columnar polycrystalline microstructures. Acta Mater. **49**, 3521 (2001)

37. Crljen, Z., Lazic, P., Sokcevic, D., Brako, R.: Relaxation and reconstruction on (111) surfaces of Au, Pt, and Cu. Phys. Rev. B **68**, 195411 (2003)

38. Takeuchi, N., Chan, C.T., Ho, K.M.: A theoretical study of the surface reconstruction and the surface electronic structure. Phys. Rev. B **43**, 13899 (1991)

39. Lozovoi, A.Y., Alavi, A.: Reconstruction of charged surfaces: General trends and a case study of Pt(110) and Au(110). Phys. Rev. B **68**, 245416 (2003)

40. Han, W.Z., Wu, S.D., Li, S.X., Zhang, Z.F.: Origin of deformation twinning from grain boundary in copper. Appl. Phys. Lett. **92**, 221909 (2008)

41. Rodrigues, V., Fuhrer, T., Ugarte, D.: Signature of atomic structure in the quantum conductance of gold nanowires. Phys. Rev. Lett. **85**, 4124 (2000)